



NASH-inducing Diets in Göttingen Minipigs

Pedersen, Henrik D.; Galsgaard, Elisabeth D.; Christoffersen, Berit; Cirera, Susanna; Holst, Dorte; Fredholm, Merete; Latta, Markus

Published in:
Journal of Clinical and Experimental Hepatology

DOI:
[10.1016/j.jceh.2019.09.004](https://doi.org/10.1016/j.jceh.2019.09.004)

Publication date:
2020

Document version
Publisher's PDF, also known as Version of record

Document license:
[CC BY-NC-ND](#)

Citation for published version (APA):
Pedersen, H. D., Galsgaard, E. D., Christoffersen, B., Cirera, S., Holst, D., Fredholm, M., & Latta, M. (2020). NASH-inducing Diets in Göttingen Minipigs. *Journal of Clinical and Experimental Hepatology*, 10(3), 211-221. <https://doi.org/10.1016/j.jceh.2019.09.004>

NASH-inducing Diets in Göttingen Minipigs

Henrik D. Pedersen^{*,†}, Elisabeth D. Galsgaard[‡], Berit Ø. Christoffersen[‡], Susanna Cirera[†],
Dorte Holst[‡], Merete Fredholm[†], Markus Latta[‡]

^{*}Ellegaard Göttingen Minipigs A/S, Dalmose, Denmark, [†]Department of Veterinary and Animal Sciences, University of Copenhagen, Denmark
and [‡]Global Drug Discovery, Novo Nordisk A/S, Maaloev, Denmark



Background: Owing to the human-like physiology, a minipig model of nonalcoholic steatohepatitis (NASH) could be valuable. Pigs, however, rarely develop substantial hepatic steatosis, even when fed diets with high fat, fructose, and cholesterol (FFC) content. The potential of choline-deficient, amino acid-defined high-fat diets (CDAHFD) was therefore evaluated in Göttingen Minipigs. **Methods:** Castrated male Göttingen Minipigs were fed either chow (n = 5) or one of the three NASH diets: FFC (n = 5), CDAHFD with sucrose (CDAHFD-S; n = 4), or fructose (CDAHFD-F; n = 4) for 8 weeks. Liver and blood samples were collected after 2 weeks and at termination. **Results:** Compared with chow, the body weight was higher after FFC (9.8 ± 0.4 versus 8.5 ± 1.2 kg; mean \pm SD) and less after CDAHFD-S (6.4 ± 0.8 kg) and CDAHFD-F (6.9 ± 0.8 kg). Liver weight per kg body weight was significantly increased in all 3 NASH groups (FFC 2.1 times; and both CDAHFD diets 3.1 times). Histologically, pronounced macrovesicular steatosis developed only in the CDAHFD groups. Inflammation was present in all three NASH groups. In the CDAHFD groups, inflammatory cells formed crown-like structures around steatotic hepatocytes. Sirius red staining revealed mild fibrosis in the two CDAHFD groups with the fibrotic potential being further supported by immunohistochemical staining for activated stellate cells and gene expression analyses. No noticeable differences were found between CDAHFD-S and CDAHFD-F. **Conclusions:** Göttingen Minipigs fed CDAHFD developed pronounced steatosis with inflammation around steatotic hepatocytes and incipient fibrosis, thereby showing potential as a model for human NASH. Further studies are needed to investigate the period needed for marked fibrosis to develop. (J CLIN EXP HEPATOL 2020;10:211–221)

Nonalcoholic fatty liver disease (NAFLD) has reached a global prevalence of 25%, with a significant number of patients progressing to nonalcoholic steatohepatitis (NASH) and potentially liver cirrhosis and hepatocellular carcinoma.¹ Histologically, the strongest predictor of disease-specific mortality is the fibrosis stage,² and the approaches for finding effective treatments for NASH include targeting the underlying metabolic disease, hepatic inflammation, and/or fibrosis.^{3,4} Good, translational animal models are instrumental for studying disease mechanisms and for drug discovery.

Pigs are more similar to humans than rodents regarding for instance metabolism, lipid profile, and in-

flammasome⁵ and are often used to model cardiovascular diseases. Furthermore, the size allows repeated tissue and blood sampling and the use of clinical diagnostic modalities. Pigs, however, rarely develop substantial hepatic steatosis, even after feeding a diet high in fat, fructose, and cholesterol (FFC) for many months^{7–11}—possibly because the liver is not the primary site of de novo lipogenesis in pigs.⁶ With regard to hepatic fibrosis, it is generally limited and varying in degree after FFC diets and tends to have a sinusoidal and periportal localization.

In rodents, choline-deficient diets are often used to induce NASH, and if factors such as the content of methionine and lipids are optimally balanced, the appetite and body weight (BW) of the animals can be maintained, significant degrees of steatosis develop quickly, and marked fibrosis can be obtained after a few months.^{12,13} Among the most promising rodent diets is the choline-deficient, L-amino acid-defined, high-fat diet (CDAHFD) with approximately 0.1% methionine and a high content of saturated fat.^{12,13} In mice, fructose in the diet leads to more hepatic fatty acid synthesis and cytotoxicity compared with glucose.^{14,15} In humans, the role of fructose *per se* in disease progression is less clear,^{14,15} and it remains to be addressed in pigs.

Keywords: Choline, Fatty liver, Fibrosis, Porcine, Animal model

Received: 6.6.2019; Accepted: 15.9.2019; Available online 21 September 2019

*Address for correspondence: Henrik D. Pedersen, Ellegaard Göttingen Minipigs A/S, Sørøe Landevej 302, 4261 Dalmose, Denmark.

E-mail: hdp@minipigs.dk

Abbreviations: NAFLD: non-alcoholic fatty liver disease; NASH: non-alcoholic steatohepatitis; FFC: high-fat, fructose, cholesterol; CDAHFD: choline-deficient; amino acid defined high-fat diet (-S: with sucrose; -F: with fructose); EDTA: ethylenediaminetetraacetic acid; GLDH: glutamate dehydrogenase; HE: hematoxylin and eosin; CD45: cluster of differentiation 45; SMA: smooth muscle actin; ALT: alanine transaminase; AST: aspartate transaminase; ALP: alkaline phosphatase; GGT: gamma-glutamyltransferase

<https://doi.org/10.1016/j.jceh.2019.09.004>

Minipigs are attractive to use in long-term studies. The Göttingen Minipig is the smallest and best characterized minipig and the one most commonly used in drug discovery worldwide.^{18,19}

The present study evaluated the potential of the following three diets to induce NASH in Göttingen Minipigs as compared with chow: FFC diet and CDAHFD with sucrose (CDAHFD-S) or fructose (CDAHFD-F).

METHODS

Animals and housing

All experiments were approved by the Danish Animal Experiments Inspectorate (license number: 2016-15-0201-01078). Eighteen male Göttingen Minipigs (Ellegaard Göttingen Minipigs, Dalmose, Denmark) were castrated at 7 weeks of age and gradually switched to their respective diets over the following week. Between 8 and 16 weeks of age, they were fed one of four diets: chow (n = 5), FFC diet (n = 5), CDAHFD-S (n = 4), or CDAHFD-F (n = 4). They were housed in groups according to diet with straw as bedding and had *ad libitum* access to fresh drinking water. The room temperature was kept at 22–24 °C and there was access to a heating lamp. Lights were on between 6 a.m. and 7 p.m. and the pigs were weighed twice weekly.

Diets and feeding

All diets were produced by Special Diets Services (Witham, United Kingdom): chow (Mini-Pig Expanded); FFC diet, containing 2% cholesterol, 0.7% cholic acid, 18% fructose, 20% fat (hydrogenated soy oil, coconut oil and lard), 0.07% choline and 0.35% methionine—matching that used in other larger minipig studies focused on NASH^{7–9}; CDAHFD, containing 1% cholesterol, 0.35% cholic acid, 30% fat (milk fat and cocoa butter), no choline, 0.1% methionine, and either 20% sucrose (CDAHFD-S) or 20% fructose (CDAHFD-F). The chow group was fed according to internal standards (3–4% of their BW per day), and the FFC group was fed the same amount of food (on weight basis). These two groups ate all the food offered. The CDAHFD groups were offered approximately 75% of this amount of food (on weight basis), i.e., an isocaloric amount relative to the chow group. All pigs were fed twice daily, with access to the food for up to 1 h each time. The minipigs in the two CDAHFD groups had decreased appetite in the beginning—a problem which was corrected over a 3- to 4-week period by adding various flavors to the diets, ending with banana cream flavor (LorAnn Oils, Lansing, MI, USA). Over the first 4 weeks, the percentages of offered diet eaten weekly were 60, 83, 81, and 93 in the CDAHFD-S group and 65, 82, 76, and 95 in the CDAHFD-F group.

Blood and liver samples

After 2 and 8 weeks of diet feeding, blood samples were taken from the jugular vein after an overnight fast. After 2 weeks on diet, each animal was furthermore anesthetized (i.m. injection of a mixture containing 0.25 mg/kg of butorphanol and 1.25 mg/kg of each of the following: tiletamine, zolazepam, ketamine, and xylazine), and had a biopsy (approximately 2 × 2 cm) surgically taken from the ventral edge of *lobus hepatis sinister medialis* by using electrosurgery shears. Each biopsy was quickly split into 3 parts, of which two were snap frozen (in tubes placed in dry ice and thereafter at –80 °C) and one was put in formalin for 4 days at 4 °C. At study end, the animals were fasted overnight, deeply anesthetized as mentioned previously and exsanguinated. The liver was quickly taken out, weighed, and photographed. Thereafter, a biopsy was taken from the middle of each of the 4 liver lobes and placed in formalin. In addition, from the middle of *lobus hepatis sinister medialis*, 4 extra samples were taken: one placed in formalin, two snap frozen on dry ice, and one placed in RNA later.

Blood analyses

After 8 weeks on diet, a hematological analysis was performed on ethylenediaminetetraacetic acid (EDTA) full blood (Advia 2120i Hematology System, Siemens, Ballerup, Denmark) and a clinical chemistry analysis was performed on serum (Advia 1800 Chemistry System). In addition, glucose, fructosamine, triglycerides, and glutamate dehydrogenase (GLDH) were measured in EDTA plasma on a Cobas 6000® autoanalyzer (Roche Diagnostics GmbH, Mannheim, Germany). Insulin and glucagon levels were measured by Luminescent Oxygen Channeling Immunoassay as previously described,²⁰ using GLU 1F120 mAb conjugated acceptor beads and biotinylated GLU 2F7 mAb for glucagon.

Biochemical analysis of liver tissue

The snap frozen liver samples (following both 2 and 8 weeks of diet feeding) were homogenized and treated as previously described.²¹ The content of cholesterol and triglycerides was measured on the Cobas 6000® autoanalyzer. For triglycerides, samples were recentrifuged after thawing and the infranatant used for analysis.

Histology

Formalin fixed samples were processed by standard procedures and stained with hematoxylin and eosin (HE) and picosirius red. Immunohistochemistry for cluster of differentiation 45 (CD45) and smooth muscle actin (SMA) was performed on the automated Discovery Ultra platform (Ventana Medical Systems, Roche, Switzerland).

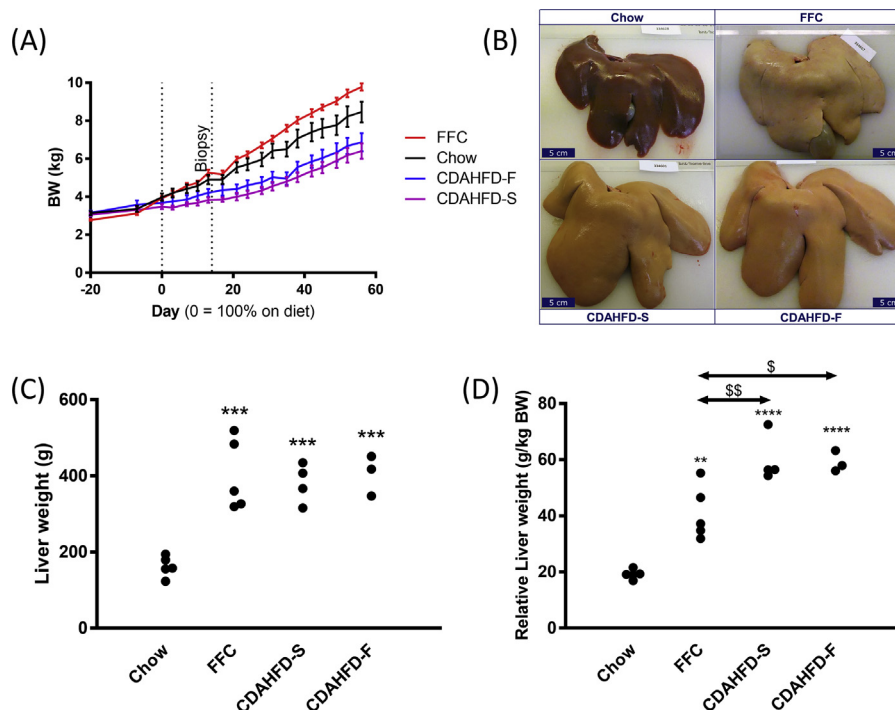


Figure 1 Body weight (A), liver gross morphology (B), liver weight (C), and relative liver weight (D) of the four different groups after 8 weeks of diet feeding: chow (n = 5), FFC (high fat, fructose and cholesterol, n = 5), CDAHFD-S (n = 4), and CDAHFD-F (n = 3); the latter two groups being choline-deficient, amino acid-defined high-fat diets with sucrose and fructose, respectively. Data in A are shown as mean \pm SEM. Scale bars in B = 5 cm. In C and D, statistically significant differences from chow (** $P < 0.01$, *** $P < 0.001$, and **** $P < 0.0001$) and between other groups (\$ $P < 0.05$, \$\$ $P < 0.01$) are indicated. CDAHFD-S, choline-deficient, amino acid-defined high-fat diet with sucrose; CDAHFD-F, choline-deficient, amino acid-defined high-fat diet with fructose.

Briefly, deparaffinized sections were subjected to heat-induced epitope retrieval using cell conditioning 1 medium for 24 min at 95 °C and blocking unspecific staining with Tris-NaCl-blocking buffer. Monoclonal rabbit anti-CD45 and the polyclonal rabbit anti-SMA antibodies (ab10588 and ab5694 from Abcam) were applied at 1 μ g/mL for 1 h at 37 °C. Antibody binding was detected with Histofine anti-rabbit universal immuno-peroxidase polymer (Nichirei Bioscience) and visualized with Purple chromogen (Roche). Nuclei were counterstained with hematoxylin. All stained sections were scanned at 20x using the NanoZoomer 2.0 HT system (Hamamatsu, Glostrup, Denmark).

Morphometry was performed with Visiopharm Integrator System (version 4.2.2.0, Visiopharm, Hoersholm, Denmark) using the acquisition module and automated image analysis, including automated tissue detection to define regions of interest. Analyses for CD45, SMA, sirius red, and nuclei were performed at 20x magnification with the preprocessing step contrast red-green followed by threshold analysis. Several postprocessing steps were performed to numerate nuclei for ratio calculations. Quantitative digital image analysis of steatosis was performed on HE sections.

Gene expression analysis

RNA was isolated from approximately 50 mg of frozen liver tissue using the RNeasy Mini Kit including DNase treatment (Qiagen, Hilden, Germany) following the manufacturer's instructions. Concentration and purity of the RNA samples were measured in a Nanodrop ND-1000 spectrophotometer (NanoDrop technologies, Wilmington, USA). RNA integrity was assessed visually with agarose gel electrophoresis and in an Experion machine using the RNA StdSens kit (BioRad, Denmark). All samples had an RNA quality index between 8.9 and 10 (average = 9.4) and were included for further processing.

Two cDNA replicates were made from each RNA sample. Briefly, 0.5 μ L ImProm-II reverse transcriptase (Promega), 0.25 μ g 1:3 OligodT/Random primers, 2 μ L ImProm-II buffer, 10 units RNasin Ribonuclease inhibitor (Promega), 2.5 mM $MgCl_2$ and 2 mM dNTP were mixed with 500 ng of RNA in a 10 μ L reaction volume. Reactions were incubated for 5 min at room temperature, 1 h at 42 °C and 15 min at 70 °C. Two negative controls were made without reverse transcriptase added. The cDNA samples were diluted 1:16 before quantitative real-time PCR (qPCR) and stored at -80 °C until use.

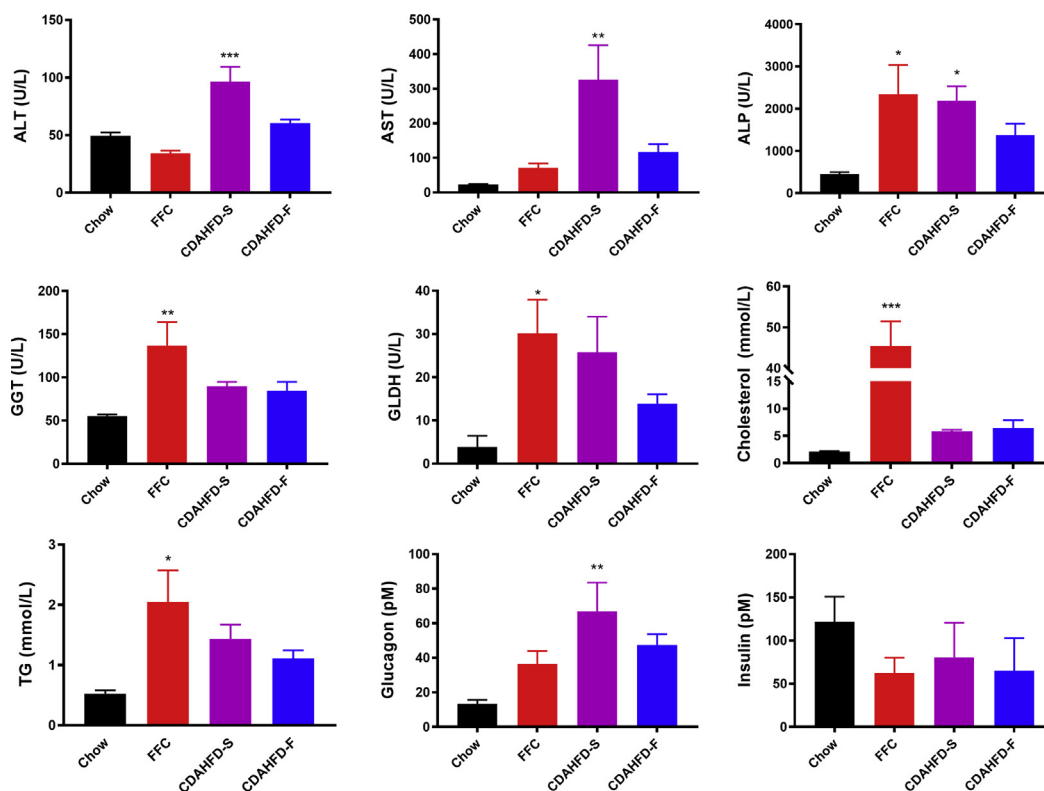


Figure 2 Selected blood biochemistry data (mean + SEM) from the four different groups after 8 weeks of diet feeding: chow ($n = 5$), FFC ($n = 5$), CDAHFD-S ($n = 4$), and CDAHFD-F ($n = 3$). Asterisks indicate statistically significant difference to chow with * $P < 0.05$, ** $P < 0.01$, and *** $P < 0.001$. ALT, alanine transaminase; AST, aspartate transaminase; ALP, alkaline phosphatase; GGT, gamma-glutamyltransferase; GLDH, glutamate dehydrogenase; TG, triglycerides; CDAHFD-S, choline-deficient, amino acid-defined high-fat diet with sucrose; CDAHFD-F, choline-deficient, amino acid-defined high-fat diet with fructose; FFC, high fat, fructose, and cholesterol.

The expression profiles of 92 genes implicated in liver metabolism and of four reference genes selected based on stable expression²² were analyzed in the study (Table S1). Primers were designed using the tool “Pick Primers” in PubMed to amplify a product in the range of 100 nucleotides, and if possible, were designed to span a large intron.

High-throughput qPCR was performed on the Biomark HD system (Fluidigm Corporation) using a 96.96 IFC chip. Fifteen cycles preamplification using TaqMan PreAmp Master Mix (Life Technologies), subsequent cleanup with Exonuclease I (New England BioLabs) and qPCR were performed according to the Fluidigm protocol using SsoFast™ EvaGreen® Supermix with Low ROX (Bio-Rad Laboratories). Standard curves were performed using a pool of the preamplified cDNA. Data were extracted using the associated software.

Statistical methods

Group comparisons were made by one-way ANOVA for BW, liver weight, blood values, and liver biochemistry data (with Tukey’s or Dunn’s multiple comparisons

tests), by Welch’s t -test for morphometric data, and by Mann-Whitney test for gene expression data. qPCR data were preprocessed using GenEx software (MultiD, Göteborg, Sweden). Briefly, data were corrected for PCR efficiency and normalized to reference genes (*ACTB*, *GAPDH*, *RPL4*, *TBP1*). The cDNA replicates were averaged, and Cq values were converted into fold changes relative to the sample with the highest Cq value for each assay, and log₂ transformed before statistical analysis. Graphs and statistical tests were made in GraphPad Prism (version 7.04, GraphPad Software Inc., La Jolla, CA, USA). Data are shown as mean \pm SEM and the significance level was $P < 0.05$, unless otherwise noted.

RESULTS

Body weight and liver weight

The CDAHFD-S group had statistically significantly lower BW at study-end compared with the chow group ($P = 0.01$). The CDAHFD-F group showed a similar trend ($P = 0.08$), whereas the FFC group tended to have a higher BW ($P = 0.10$; Figure 1A).

Table 1 Hematological and Blood Biochemical Parameters.

Parameter	Chow	FFC	CDAHFD-S	CDAHFD-F
Leucocytes ($10^9/L$)	9.9 ± 1.0	17.2 ± 2.6	12.7 ± 1.8	13.0 ± 2.1
Erythrocytes ($10^{12}/L$)	8.7 ± 0.3	7.6 ± 0.2	$6.0 \pm 0.7^{**}$	$6.7 \pm 0.5^*$
Hemoglobin (mmol/L)	7.9 ± 0.3	6.5 ± 0.3	$6.0 \pm 0.6^*$	6.4 ± 0.6
Hematocrit (%)	42 ± 2	35 ± 2	$30 \pm 3^*$	34 ± 4
Thrombocytes ($10^9/L$)	284 ± 80	392 ± 48	207 ± 67	199 ± 98
Neutrophils ($10^9/L$)	1.6 ± 0.4	3.6 ± 0.6	3.4 ± 0.5	$4.9 \pm 1.0^{**}$
Lymphocytes ($10^9/L$)	7.4 ± 0.7	11.2 ± 1.5	7.7 ± 1.2	6.4 ± 1.1
Monocytes ($10^9/L$)	0.28 ± 0.06	0.79 ± 0.22	0.57 ± 0.21	0.52 ± 0.10
Eosinophils ($10^9/L$)	0.51 ± 0.22	1.24 ± 0.36	0.78 ± 0.16	0.87 ± 0.14
Basophils ($10^9/L$)	0.03 ± 0.01	0.05 ± 0.01	0.02 ± 0.01	0.03 ± 0.01
Reticulocytes ($10^9/L$)	128 ± 10	123 ± 16	$389 \pm 122^*$	275 ± 52
Creatine kinase (U/L)	243 ± 30	452 ± 204	715 ± 431	289 ± 29
Total bilirubin ($\mu\text{mol/L}$)	0.0 ± 0.0	1.2 ± 0.4	$6.0 \pm 1.7^{**}$	2.0 ± 1.5
Urea (mmol/L)	3.0 ± 0.2	2.8 ± 0.3	$4.2 \pm 0.4^*$	3.8 ± 0.1
Creatinine ($\mu\text{mol/L}$)	91.0 ± 4.4	$69.2 \pm 4.1^{**}$	$51.8 \pm 4.6^{***}$	$56.0 \pm 5.6^{***}$
Albumin (g/L)	40.6 ± 1.7	39.8 ± 1.1	41.3 ± 1.1	44.0 ± 1.8
Total protein (g/L)	54.9 ± 1.0	59.5 ± 1.5	57.2 ± 1.2	$61.4 \pm 1.5^*$
Iron ($\mu\text{mol/L}$)	42.3 ± 6.7	30.6 ± 2.6	30.4 ± 3.0	26.5 ± 5.6
Phosphate (mmol/L)	2.34 ± 0.06	$2.82 \pm 0.08^{***}$	$2.68 \pm 0.03^{**}$	$2.87 \pm 0.03^{***}$
Calcium (mmol/L)	2.86 ± 0.06	2.77 ± 0.07	2.88 ± 0.08	2.93 ± 0.03
Magnesium (mmol/L)	1.03 ± 0.03	1.01 ± 0.06	0.96 ± 0.02	1.02 ± 0.05
Sodium (mmol/L)	146.7 ± 0.9	143.4 ± 2.1	142.7 ± 1.3	144.7 ± 0.8
Potassium (mmol/L)	4.8 ± 0.3	4.9 ± 0.2	5.3 ± 0.2	5.8 ± 0.2
Globulin (g/L)	14.3 ± 0.8	$19.7 \pm 0.7^{***}$	15.8 ± 0.6	17.4 ± 1.0
Fructosamine ($\mu\text{mol/L}$)	228 ± 4	238 ± 12	245 ± 6	242 ± 5
Glucose (mmol/L)	4.9 ± 0.3	4.3 ± 0.3	4.6 ± 0.3	5.4 ± 0.8

Data are mean \pm SEM. * $P < 0.05$ vs chow, ** $P < 0.01$ vs chow, *** $P < 0.001$ vs chow.

CDAHFD-S, choline-deficient, amino acid-defined high-fat diet with sucrose; CDAHFD-F, choline-deficient, amino acid-defined high-fat diet with fructose; FFC, high fat, fructose, and cholesterol.

Compared with the chow group, the liver was large and pale in all minipigs from the three NASH groups (Figure 1B) and weighed more (chow 162 ± 12 g; FFC 402 ± 42 g; CDAHFD-S 381 ± 26 g; CDAHFD-F 405 ± 31 g; all $P < 0.001$; Figure 1C). Compared with a mean relative liver weight of 19.2 g/kg in the chow group, that of the FFC group was increased 2.1-fold (41.1 g/kg), the CDAHFD-S group 3.1-fold (59.9 g/kg), and the CDAHFD-F group 3.1-fold (59.0 g/kg), as shown in Figure 1D. One minipig in the CDAHFD-F group had subdued behavior and inappetence two weeks before study-end and was euthanized for ethical reasons. At necropsy, the gastrointestinal system of this pig showed signs of ileus. The liver gross and histological appearance and weight was like the other CDAHFD-F minipigs (data not shown). No study-end data from this minipig were included in any analyses. Splenomegaly with a pale appear-

ance was found in all animals in the FFC group (Fig. S1). Histologically, an accumulation of foamy macrophage-like cells was seen in these spleens (Fig. S2).

Hematological and biochemical blood tests

Except from alanine transaminase, all other biomarkers of liver damage (AST, aspartate transaminase; ALP, alkaline phosphatase; GGT, gamma-glutamyltransferase and GLDH glutamate dehydrogenase) were increased in all three NASH groups, albeit not statically significantly in all cases (Figure 2). The markers of dyslipidemia (triglyceride and cholesterol) were increased in all the NASH groups, albeit only statistically significantly in the FFC group. Neither blood glucose (Table 1) nor plasma insulin levels changed significantly over the course of 8 weeks, whereas plasma glucagon was significantly increased in the

CDAHFD-S group and showed a similar trend in the other two NASH groups.

With regard to other blood parameters, the CDAHFD-S group had decreased erythrocytes, hemoglobin, and hematocrit, and increased reticulocytes, suggestive of mild regenerative anemia (Table 1). The FFC group had elevated globulin levels, the CDAHFD-F group had elevated number of neutrophils, and all three NASH groups had elevated plasma phosphate concentrations and decreased plasma creatinine concentrations (Table 1). The remaining parameters were not significantly altered by diet.

Biochemical analyses of liver tissue

The triglyceride content in the liver of the minipigs was similar in the chow and FFC group, but it was markedly increased in the two CDAHFD groups—a change that was seen already in the 2-week samples (Figure 3). The cholesterol content in the liver was significantly increased in all three NASH groups already after 2 weeks, and remained high after 8 weeks, although not statistically significant in the FFC group ($P = 0.08$).

Histology

Based on HE staining, pronounced steatosis was observed throughout the parenchyma in both CDAHFD groups,

with markedly larger lipid droplets after 8 weeks than after 2 weeks (Figure 4). When quantified by morphometry, the two CDAHFD groups showed increased hepatic steatosis already at week 2 which was further augmented at week 8, with no difference between CDAHFD-S and CDAHFD-F (Figure 5A and B). Hepatic steatosis was not present in the FFC group, but “foamy” macrophage-like cells lining the sinusoids were noticed (Figures 4, 5A and B). No evidence of ballooning degeneration was observed in any of the minipigs.

Lobular inflammatory foci were observed in the 2- and 8-week liver samples from both CDAHFD groups, but not in the FFC group (Figure 4A and B). CD45 is a marker for leukocytes and immunohistochemical staining confirmed the presence of both resident Kupffer cells and patrolling immune cells in livers from chow animals (Figure 4B). Morphologically, crown-like structures around single, fatty hepatocytes were present in the CDAHFD groups, indicating the presence of microgranulomas (Figure 4B). These structures were not observed in the FFC group, in which sinusoidal foamy macrophage-like cells were seen instead (Figure 4A and B). Morphometric quantification showed significantly increased CD45 staining in all three NASH groups compared with chow (Figure 5C).

Activation of hepatic stellate cells was visualized in 8-week samples by SMA immunohistochemistry. In both

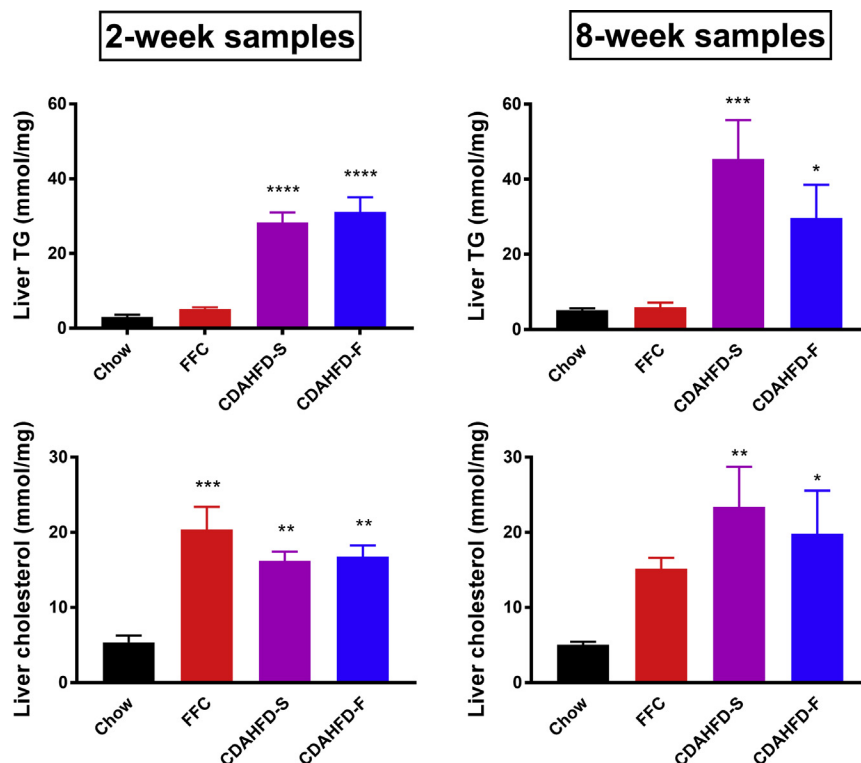


Figure 3 Content of triglycerides (TG; upper panels) and total cholesterol (lower panels) in liver samples taken after two and eight weeks of diet feeding with chow ($n = 5$), FFC ($n = 5$), CDAHFD-S ($n = 4$), and CDAHFD-F ($n = 3$). Data are shown as mean + SEM. Asterisks indicate statistically significantly different from chow with * $P < 0.05$, ** $P < 0.01$, *** $P < 0.001$, and **** $P < 0.0001$. CDAHFD-S, choline-deficient, amino acid-defined high-fat diet with sucrose; CDAHFD-F, choline-deficient, amino acid-defined high-fat diet with fructose; FFC, high fat, fructose, and cholesterol.

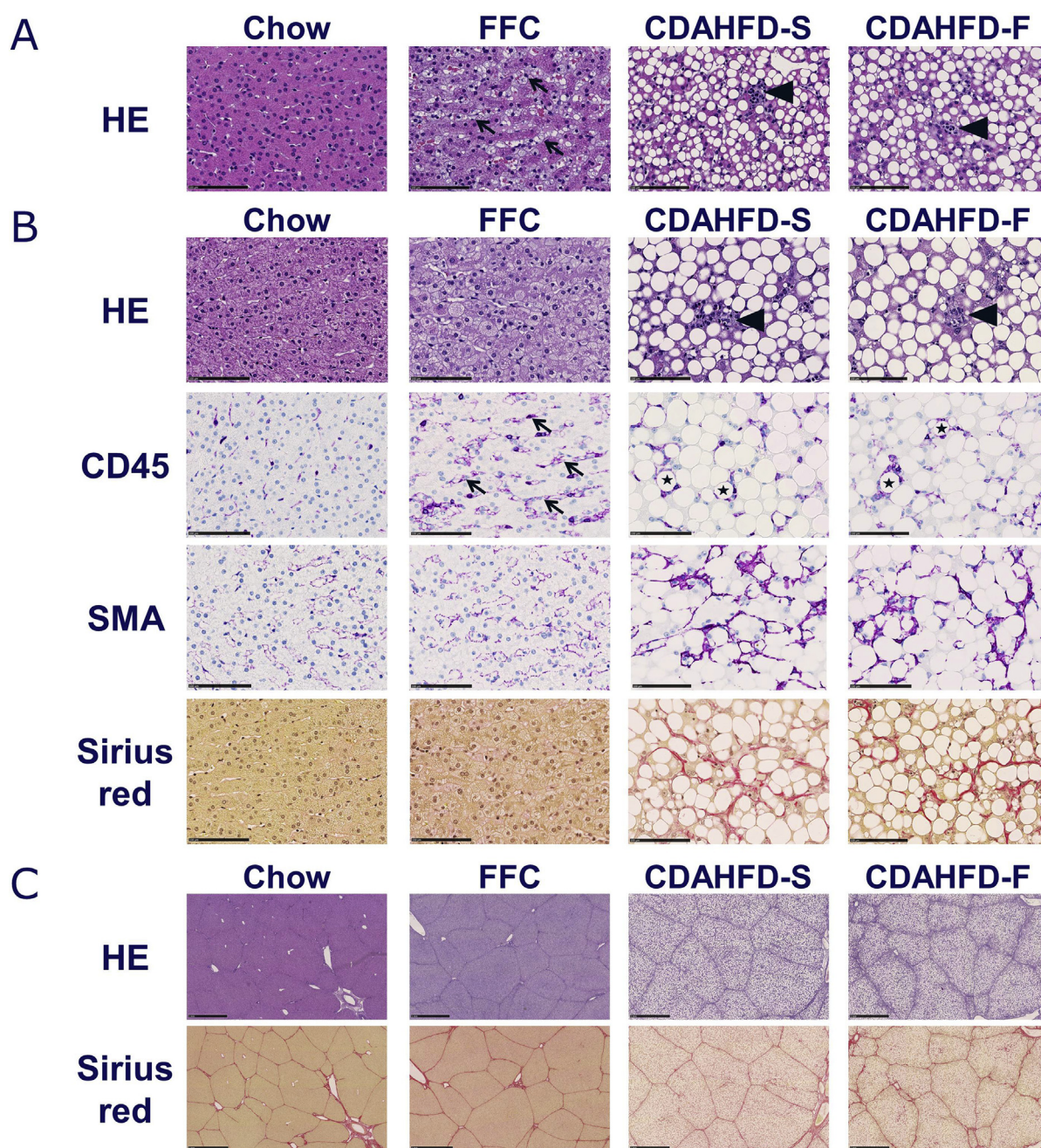


Figure 4 Histological analyses of liver samples from Göttingen Minipigs after 2 (A) and 8 (B, C) weeks of feeding with the indicated diets: chow, FFC, CDAHFD-S, and CDAHFD-F. Representative pictures show HE staining (upper panels in A, B, C), immunohistochemistry for CD45 and SMA (middle panels in B) and sirius red staining (lower panels in B, C). Arrows, arrow heads, and asterisks indicate sinusoidal foamy macrophages, inflammatory foci, and crown-like structures, respectively. Scale bars = 100 μ m (A, B) and 1 mm (C). CDAHFD-S, choline-deficient, amino acid-defined high-fat diet with sucrose; CDAHFD-F, choline-deficient, amino acid-defined high-fat diet with fructose; FFC, high fat, fructose, and cholesterol; CD45, cluster of differentiation 45; SMA, smooth muscle actin.

CDAHFD groups, strong SMA staining was observed perisinusoidally, in between, and surrounding steatotic hepatocytes (Figure 4B). When quantified by morphometry, SMA stained area was statistically significantly higher in the two CDAHFD groups than in the chow and FFC groups (Figure 5D). SMA area was increased only weakly

in the FFC group compared with chow and localized perisinusoidally like the SMA-positive cells in the chow group (Figures 4B and 5D).

Fibrosis assessed morphometrically from sirius red stained samples was statistically significantly increased in both CDAHFD groups compared with chow, whereas no

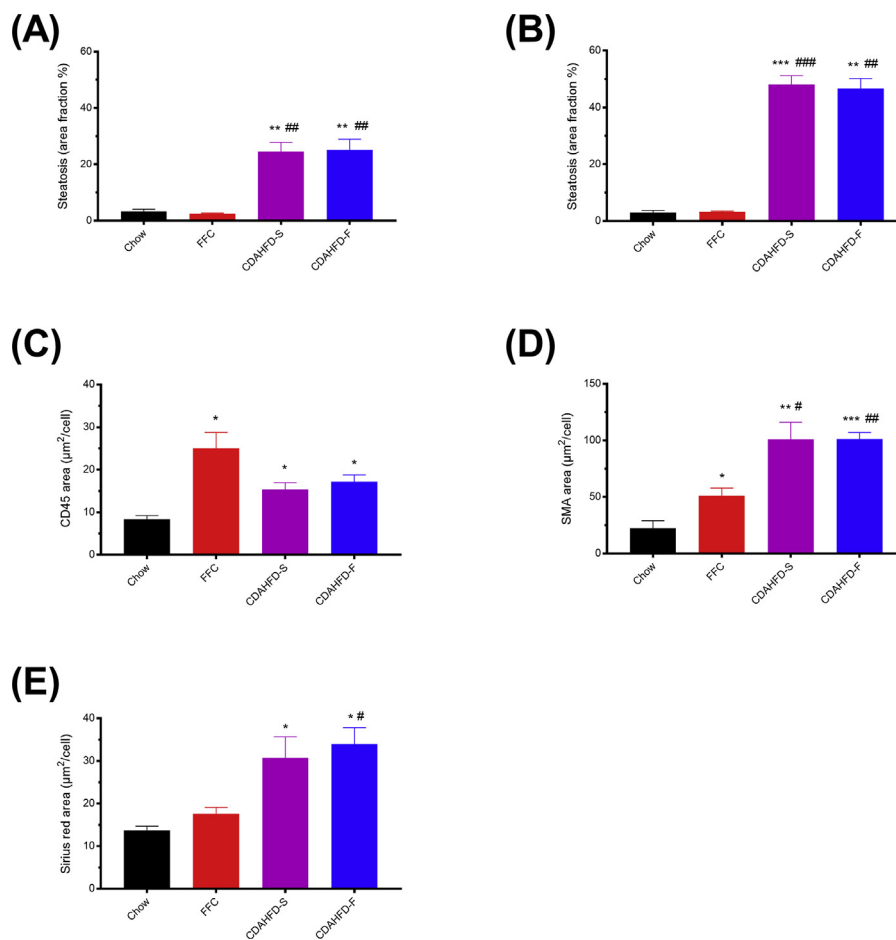


Figure 5 Morphometric assessment of steatosis (A, B), CD45 (C), smooth muscle actin (SMA) (D), and sirius red (E) staining in livers from Göttingen Minipigs after 2 (A) and 8 (B–E) weeks of feeding with different diets: chow (n = 5), FFC (n = 5), CDAHFD-S (n = 4), and CDAHFD-F (n = 3). Data are shown as mean + SEM. * and # $P < 0.05$ vs chow and FFC, respectively, ** and ## $P < 0.01$ vs chow and FFC, respectively, *** and ### $P < 0.001$ vs chow and FFC, respectively. CD45, cluster of differentiation 45; CDAHFD-S, choline-deficient, amino acid-defined high-fat diet with sucrose; CDAHFD-F, choline-deficient, amino acid-defined high-fat diet with fructose; FFC, high fat, fructose, and cholesterol.

increase was observed in the FFC group (Figure 5E). The fibrotic tissue in the CDAHFD groups formed a chicken-wire pattern around steatotic hepatocytes mirroring the localization of SMA⁺ cells (Figure 4B). In contrast to human livers, porcine liver lobules are surrounded by distinct collagen septae which appeared unchanged in all three NASH groups compared with chow (Figure 4C).

Gene expression

When compared with the chow group, many genes showed statistically significantly different expression in the three NASH groups (Tables S2 and S3 and Figure 6), especially at the 8-week time point. Figure 6A shows expression of genes involved in de novo fibrogenesis (*COL1A1*, *COL3A1*); reorganization of extracellular matrix (*MMP9*, *TIMP1*); and stellate cell activation (*ACTA2*) after 8 weeks. The expression of *COL1A1* and *COL3A1* was significantly increased in the two CDAHFD groups, and the expression

of *MMP9* and *TIMP1* was significantly increased in all three NASH groups. *ACTA2* was significantly upregulated in the CDAHFD-F group and showed a similar tendency in the CDAHFD-S group ($P = 0.06$).

Figure 6B represents genes encoding proteins associated with inflammation, such as cytokines (*CCL2*, *IL6*, and *TNFA*), *TLR4*, and *CD68* (a marker of macrophages and Kupffer cells). Overall, these genes had significantly increased expression in all three NASH groups compared with the chow group.

Figure 6C illustrates genes encoding proteins involved in lipid, bile, and cholesterol metabolism. All three NASH groups had significantly increased expression of *CD36*, *CYP7A1*, and *LPL*; and significantly decreased expression of *HMGCR*, *LDLR*, and *PCSK9*. The NASH groups differed markedly regarding *FABP4* gene expression, which was unaltered in the FFC group but significantly increased in the two CDAHFD groups (see also Table S2).

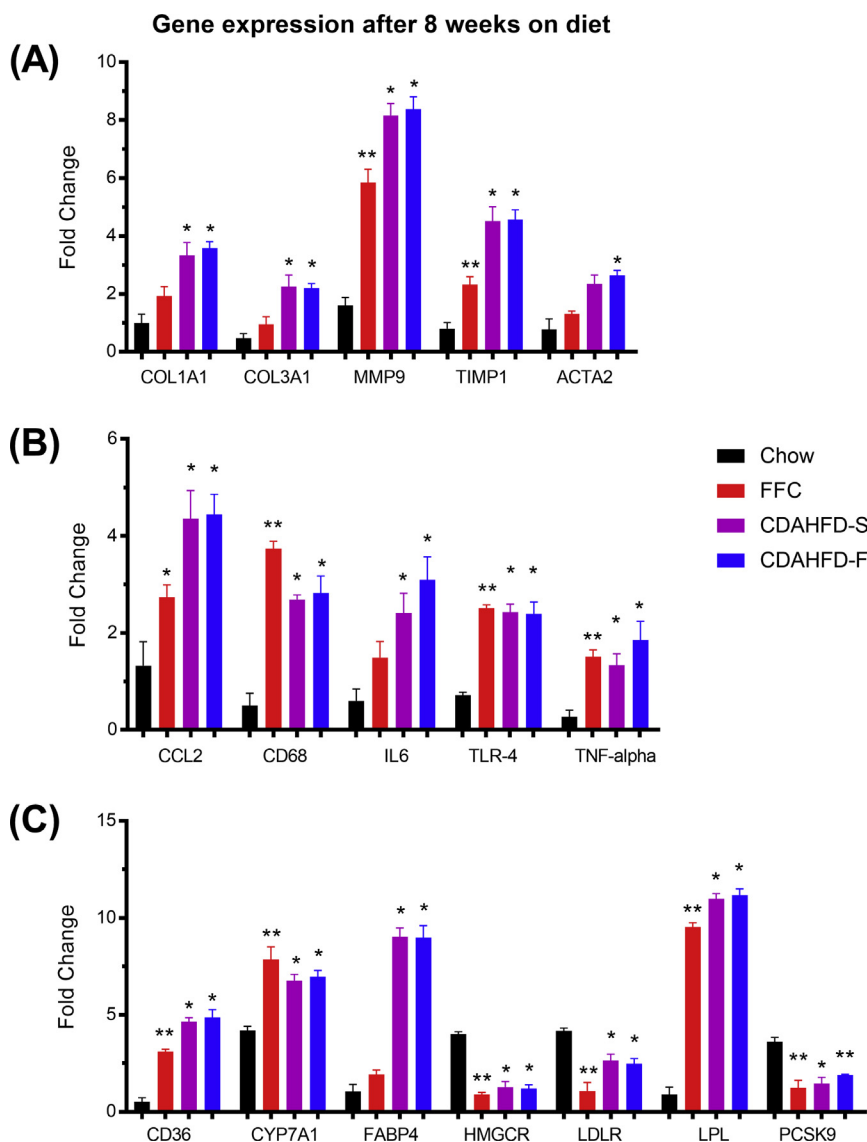


Figure 6 Hepatic mRNA levels for genes associated with fibrosis (A), inflammation (B), and lipid metabolism (C) after 8 weeks of feeding Göttingen Minipigs with different diets: chow (n = 5), FFC (n = 5), CDAHFD-S (n = 4), and CDAHFD-F (n = 3). The data were normalized to a panel of four stable reference genes and are represented as means + SEM of the fold changes for each diet group. * $P < 0.05$ vs chow, ** $P < 0.01$ vs chow. *ACTA2*, smooth muscle α -2 actin; *CCL2*, chemokine (C–C motif) ligand 2; *CD36*, cluster of differentiation (CD) 36; *CD68*, cluster of differentiation 68; *COL1A1*, alpha-1 type I collagen; *COL3A1*, alpha-1 type III collagen; *CYP7A1*, cytochrome P450 family 7 subfamily A member 1; *FABP4*, fatty acid-binding protein 4; *HMGCR*, 3-hydroxy-3-methylglutaryl-CoA reductase; *IL6*, interleukin-6; *LDLR*, low-density lipoprotein receptor; *LPL*, lipoprotein lipase; *MMP9*, matrix metalloproteinase-9; *PCSK9*, proprotein convertase subtilisin/kexin type 9; *TIMP1*, metalloproteinase inhibitor 1; *TLR4*, toll-like receptor 4; *TNFA*, tumor necrosis factor alpha; CDAHFD-S, choline-deficient, amino acid-defined high-fat diet with sucrose; CDAHFD-F, choline-deficient, amino acid-defined high-fat diet with fructose; FFC, high fat, fructose, and cholesterol.

DISCUSSION

Göttingen Minipigs fed CDAHFD for 8 weeks developed widespread and pronounced hepatic steatosis with lobular inflammatory foci, activated stellate cells, increased expression of profibrotic genes, and fibrosis in a chicken-wire pattern associated with steatotic hepatocytes. In line with other minipig studies, FFC diet did not cause significant steatosis after 8 weeks, at which time point inflammation was dominated by foamy macrophage-like cells.

The low variation within the CDAHFD groups in the present study indicates a more robust and reproducible model than that described in previous studies with FFC diet. It appears that the content of methionine and lipids was optimal in the CDAHFD diets, as it was possible to obtain a growth rate on par with that in the chow group in the last half of the study (after addition of flavor to the diet). Although the minipigs on CDAHFD were not obese, their plasma triglyceride and cholesterol levels were slightly elevated. Despite the changes in diet

composition, however, none of the NASH groups showed signs of significant insulin resistance, as they all had normal levels of glucose and fructosamine (a measure of long-term glucose levels), and low-to-normal insulin levels. The low creatinine concentrations in all NASH groups probably reflect impaired liver function.²³ Among the circulating liver damage markers, ALP and GLDH were the most consistently increased in the NASH groups, and thus show some potential as biomarkers.

Pronounced macrovesicular steatosis was established already after 2 weeks on CDAHFD and was even more manifest after 8 weeks. Choline deficiency induces steatosis by impairing hepatic Very Low Density Lipoproteins (VLDL) export. The FFC group did not display appreciable steatosis—in agreement with long-term studies with a similar diet.^{7–9} Species differences in localization of de novo lipogenesis might contribute to this.⁶ Thus, FFC diets (or similar) will not cause marked steatosis (and steatosis-driven inflammation and fibrosis) in pigs. However, we observed foamy macrophage-like cells in both liver and spleen of the minipigs in the FFC group, as previously reported.¹¹ Increased gene expression of *FABP4*, *CD36*, and *LPL* indicates increased fatty acid uptake, transport, and metabolism in the NASH groups, and the fact that *FABP4* only showed a statistically significantly increased expression in the two CDAHFD groups reflects that only these groups had hepatic steatosis. The dietary cholesterol repressed the endogenous cholesterol synthesis (reduced *HMGCR*), increased the cholesterol metabolism (increased *CYP7A1*), and increased the hepatic uptake of circulating cholesterol (reduced *PCSK9*) in all the NASH groups.

Foci of inflammatory cells were seen already after 2 weeks in the CDAHFD groups. The morphometric CD45 immunohistochemistry data showed that all NASH groups had an increased number of inflammatory cells compared with the chow group after both 2 and 8 weeks. These cells were localized sinusoidally in the FFC group, presumably representing foamy macrophages, whereas they formed crown-like structures around steatotic hepatocytes in the two CDAHFD groups. Such crown-like structures are seen in mouse models and in humans with NASH and are suggested to be an important indicator of disease progression from simple steatosis to NASH.²⁴ In line with the histology findings, the expression of *CD68* was increased in all NASH groups, supporting recruitment of proinflammatory monocytes/macrophages and/or activation of resident Kupffer cells.

Histologically, fibrosis as evaluated by sirius red staining was present in the CDAHFD groups after 8 weeks forming a chicken-wire pattern associated with steatotic hepatocytes. When quantified by morphometry, sirius red data showed significantly increased fibrosis in the CDAHFD groups. In accordance with this, quantitative analysis of IHC staining for SMA, a marker of fibrinogenic myofibroblast such as activated stellate cells, showed

increased levels in the NASH groups and especially so in the two CDAHFD groups and, moreover, the gene expression analyses showed that genes associated with fibrosis were expressed at higher levels in these groups and less so in the FFC group. The importance of these genes in human NASH was recently shown.^{4,25–27} The CDAHFD groups thus showed more evidence of ongoing profibrotic processes, and in addition, the fibrosis appeared to be driven by the steatotic hepatocytes like in humans.

Fibrosis was recently found to be the only histological feature with prognostic importance in human NAFLD,² and a number of pharmaceutical companies are pursuing antifibrotic targets.^{3,4} In that connection, a Göttingen Minipig NASH model based on CDAHFD could be valuable. Notably, the minipig has a more human-like metabolism, lipid profile, and inflammasome⁵ than rodents—as well as a size allowing repeated tissue and blood sampling. The level of fibrosis seen already at 8 weeks of diet feeding gives hope that the model over time could develop true bridging fibrosis, which typically cannot be obtained in steatosis-driven steatohepatitis in mice. It appears that several months will be needed for severe fibrosis to develop, and this is a disadvantage of the model. However, significant information about disease development can be gained early on by following disease markers such as gene expression patterns.

The sugar source did not significantly influence the findings in the CDAHFD groups in this study. In mice, fructose leads to more hepatic fatty acid synthesis and cytotoxicity than glucose.^{14,15} In humans, the evidence of harmful effects of fructose, in isocaloric amounts, is less clear.^{16,17}

Göttingen Minipigs fed CDAHFD for 8 weeks developed pronounced steatosis with inflammation and fibrosis associated with steatotic hepatocytes. In concert with previous minipig studies, FFC diet did not produce steatosis and there was no significant fibrosis. The CDAHFD diets described here show promise as a basis for a minipig NASH model with human-like dyslipidemia and hence with high translational value. Long-term studies are warranted to show the period needed for marked fibrosis to develop.

CONFLICTS OF INTEREST

HDP is full time employed at Ellegaard Göttingen Minipigs A/S.

ACKNOWLEDGEMENTS

The authors thank Adrian Zeltner, Gitte Billskog Hansen, Carina Christoffersen, Pernille Birch, Pia Skårup Andersen, Malik Nygaard Nielsen, Thit Tjagvad, Susanne Juul Rasmussen, Jette Mandelbaum, Pia Rothe, Louise Degn Agerholm, Hanne Toftelund, Johnny Kaltoft Nisted, Lotte

Schmidt Marcher, and Tina N. Mahler for excellent technical assistance; Johannes Josef Fels from Novo Nordisk for analyzing insulin and glucagon.

FUNDING

Ellegaard Göttingen Minipigs A/S funded the *in vivo* part of the study, and the subsequent analyses of tissue and blood were funded by Copenhagen University (gene expression analyses) and Novo Nordisk A/S (remaining analyses).

REFERENCES

1. Younossi ZM, Koenig AB, Abdelatif D, Fazel Y, Henry L, Wymer M. Global epidemiology of nonalcoholic fatty liver disease-Meta-analytic assessment of prevalence, incidence, and outcomes. *Hepatology*. 2016;64:73–84.
2. Ekstedt M, Hagstrom H, Nasr P, et al. Fibrosis stage is the strongest predictor for disease-specific mortality in NAFLD after up to 33 years of follow-up. *Hepatology*. 2015;61:1547–1554.
3. Musso G, Cassader M, Gambino R. Non-alcoholic steatohepatitis: emerging molecular targets and therapeutic strategies. *Nat Rev Drug Discov*. 2016;15:249–274.
4. Tsuchida T, Friedman S. Mechanism of hepatic stellate cell activation. *Nat Rev Gastroenterol Hepatol*. 2017;14:397–411.
5. Dawson HD, Smith AD, Chen C, Urban Jr JF. An in-depth comparison of the porcine, murine and human inflammasomes; lessons from the porcine genome and transcriptome. *Vet Microbiol*. 2017;202:2–15.
6. Bergen WG, Mersmann HJ. Comparative aspects of lipid metabolism: impact on contemporary research and use of animal models. *J Nutr*. 2005;135:2499–2502.
7. Schumacher-Petersen C, Christoffersen B, Kirk RK, et al. Experimental non-alcoholic steatohepatitis in Göttingen Minipigs: consequences of high fat-fructose-cholesterol diet and diabetes. *J Transl Med*. 2019;17:110.
8. Lee L, Alloosh M, Saxena R, et al. Nutritional model of steatohepatitis and metabolic syndrome in the Ossabaw miniature swine. *Hepatology*. 2009;50:56–67.
9. Liang T, Alloosh M, Bell LN, et al. Liver injury and fibrosis induced by dietary challenge in the Ossabaw miniature Swine. *PLoS One*. 2015 <https://doi.org/10.1371/journal.pone.0124173>.
10. Yang SL, Xia JH, Zhang YY, et al. Hyperinsulinemia shifted energy supply from glucose to ketone bodies in early nonalcoholic steatohepatitis from high-fat high-sucrose diet induced Bama minipigs. *Sci Rep*. 2015;5:13980.
11. Yamada S, Kawaguchi H, Yamada T, et al. Cholic acid enhances visceral adiposity, atherosclerosis and nonalcoholic fatty liver disease in microminipigs. *J Atheroscler Thromb*. 2017;24:1150–1166.
12. Matsumoto M, Hada N, Sakamaki Y, et al. An improved mouse model that rapidly develops fibrosis in non-alcoholic steatohepatitis. *Int J Exp Pathol*. 2013;94:93–103.
13. Chiba T, Suzuki S, Sato Y, Itoh T, Umegaki K. Evaluation of methionine content in a high-fat and choline-deficient diet on body weight gain and the development of non-alcoholic steatohepatitis in mice. *PLoS One*. 2016 <https://doi.org/10.1371/journal.pone.0164191>.
14. Pickens MK, Ogata H, Soon RK, Grenert JP, Maher JJ. Dietary fructose exacerbates hepatocellular injury when incorporated into a methionine-choline-deficient diet. *Liver Int*. 2010;30:1229–1239.
15. Softic S, Gupta MK, Wang GX, et al. Divergent effects of glucose and fructose on hepatic lipogenesis and insulin signaling. *J Clin Invest*. 2017;127:4059–4074.
16. Rippe JM, Angelopoulos TJ. Sucrose, high-fructose corn syrup, and fructose, their metabolism and potential health effects: what do we really know? *Adv Nutr*. 2013;4:236–245.
17. Ter Horst KW, Serlie MJ. Fructose consumption, lipogenesis, and non-alcoholic fatty liver disease. *Nutrients*. 2017;9:981.
18. Swindle MM. Biology, handling, husbandry and anatomy. In: Swindle MM, ed. *Swine in the Laboratory: Surgery, Anesthesia, Imaging, and Experimental Techniques*. 2nd ed. Boca Raton, FL: CRC Press; 2007:1–33.
19. Forster R, Bode G, Ellegaard L, van der Laan JW. The RETHINK project - minipigs as models for the toxicity testing of new medicines and chemicals: an impact assessment. *J Pharmacol Toxicol Methods*. 2010;62:158–159.
20. Haagenen AM, Sørensen DB, Sandue P, et al. High fat, low carbohydrate diet limit fear and aggression in Göttingen minipigs. *PLoS One*. 2014 <https://doi.org/10.1371/journal.pone.0093821>.
21. Tveden-Nyborg P, Birck MM, Ipsen DH, et al. Diet-induced dyslipidemia leads to nonalcoholic fatty liver disease and oxidative stress in Guinea pigs. *Transl Res*. 2016;168:146–160.
22. Nygard AB, Jørgensen CB, Cirera S, Fredholm M. Selection of reference genes for gene expression studies in pig tissues using SYBR green qPCR. *BMC Mol Biol*. 2007;8:67.
23. Cocchetto DM, Tschanz C, Bjornsson TD. Decreased rate of creatinine production in patients with hepatic disease: implications for estimation of creatinine clearance. *Ther Drug Monit*. 1983;5:161–168.
24. Itoh M, Kato H, Suganami T, et al. Hepatic crown-like structure: a unique histological feature in non-alcoholic steatohepatitis in mice and humans. *PLoS One*. 2013 <https://doi.org/10.1371/journal.pone.0082163>.
25. Murphy SK, Yang H, Moylan CA, et al. Relationship between methylome and transcriptome in patients with nonalcoholic fatty liver disease. *Gastroenterology*. 2013;145:1076–1087.
26. Moylan CA, Pang H, Dellinger A, et al. Hepatic gene expression profiles differentiate presymptomatic patients with mild versus severe nonalcoholic fatty liver disease. *Hepatology*. 2014;59:471–482.
27. Munsterman ID, Kendall T, Khelil N, et al. Extracellular matrix components indicate remodelling activity in different fibrosis stages of human non-alcoholic fatty liver disease. *Histopathology*. 2018 <https://doi.org/10.1111/his.13665>.

SUPPLEMENTARY DATA

Supplementary data to this article can be found online at <https://doi.org/10.1016/j.jceh.2019.09.004>.